Performance Evaluation of Coexistence within Wireless Personal Area Networks

APPROVED BY

SUPERVISING COMMITTEE:

Brian L. Evans, Supervisor

Haris Vikalo

Performance Evaluation of Coexistence within Wireless Personal Area Networks

by

Ghadi Sebaali, B.E.

REPORT

Presented to the Faculty of the Graduate School of

The University of Texas at Austin

in Partial Fulfillment

of the Requirements

for the Degree of

MASTER OF SCIENCE IN ENGINEERING

THE UNIVERSITY OF TEXAS AT AUSTIN

December 2016

Dedicated to my parents, brother, sister, uncles and grandparents.

Acknowledgments

I would like to thank my advisor Prof. Brian L. Evans for his comments on this report throughout this semester and for his guidance and help throughout my studies here at UT Austin. I am very indebted to his supervision and help. I also thank Prof. Haris Vikalo for reading this report and for being an inspiring teacher. I also would like to express special thanks to Melanie Gulick for her amazing kindness, support and help and for Pablo Caballero for his feedback on this report and for all the help and support.

Performance Evaluation of Coexistence within Wireless Personal Area Networks

Ghadi Sebaali, M.S.E.
The University of Texas at Austin, 2016

Supervisor: Brian L. Evans

With the growing interest in the Internet of Things, unlicensed frequency bands are becoming congested by an increasing number of wireless devices governed by different standards. As a result, the communication performance between transmitters and their intended receivers deteriorates. This report targets the evaluation of coexistence for selected Wireless Personal Area Network standards using simulation and experimental approaches.

Table of Contents

List of Tables

List of Figures

List of Abbreviations

AGC .... Automatic Gain Control
AFH .... Adaptive Frequency Hopping
BER .... Bit Error Rate
BLE .... Bluetooth Low Energy
BPSK .... Binary Phase Shift Keying
CCA .... Clear Channel Assessment
CSM .... Common Signaling Mode
DSSS .... Direct Sequence Spread Spectrum
DUR .... Desired-to-Undesired Ratio
DQPSK ...... Differential Quadrature Phase Shift Keying
DPSK .... Differential Phase Shift Keying
EB .... Enhanced Beacon
FEC .... Forward Error Correction
FER .... Frame Error Rate
FFT .... Fast Fourier Transform
FHSS .... Frequency Hopping Spread Spectrum
FSK .... Frequency Shift Keying
GFSK .... Gaussian Frequency Shift Keying
IAR .... Ingenjorsfirman Anders Rundgren
ISM .... Industrial, Scientific and Medical
MCS .... Modulation Coding Scheme

MPM .... Multi PHY Management

MXG .... Microwave Analog Signal Generator

O-QPSK ..... Orthogonal Quadrature Phase Shift Keying

PER .... Packet Error Rate

PHY .... Physical

PL .... Path Loss

QAM .... Quadrature Amplitude Modulation

QoS .... Quality of Service

RF .... Radio Frequency

RSS .... Received Signal Strength

R&S SMBV . Rohde & Schwarz Vector Signal Generator

SNR .... Signal to Noise Ratio (SNR)

TDM .... Time Division Multiplexing

Chapter 1

Introduction

With the growing interest in the Internet of Things, frequency bands are becoming congested by an increasing number of wireless devices governed by different standards. According to Cisco's forecast in Fig. 1.1, there will be over 11.6 billion connected devices in 2020 operating under different standards for purposes of cellular, Wi-Fi and other connectivity. As a result, communication performance between transmitters and their intended receivers is deteriorated and the data throughput and reliability are decreased. In fact, operation of multiple standards in the same frequency band leads to an increase in packet loss rates. In Wi-Fi, for example, packet rate loss is about 90% for file transfer and 30% for video streaming [3] in the presence of other wireless technologies compared to 3 -10% in Bluetooth [4] under interference. In order to ensure reliable communication between different technologies to meet the higher demand in data throughput rates, it is important to the development as well as to the operation to account for interference. This is done through simulation and more importantly through measuring the performance of radios on the physical layer level in the practical world in the presence of other interfering standards.

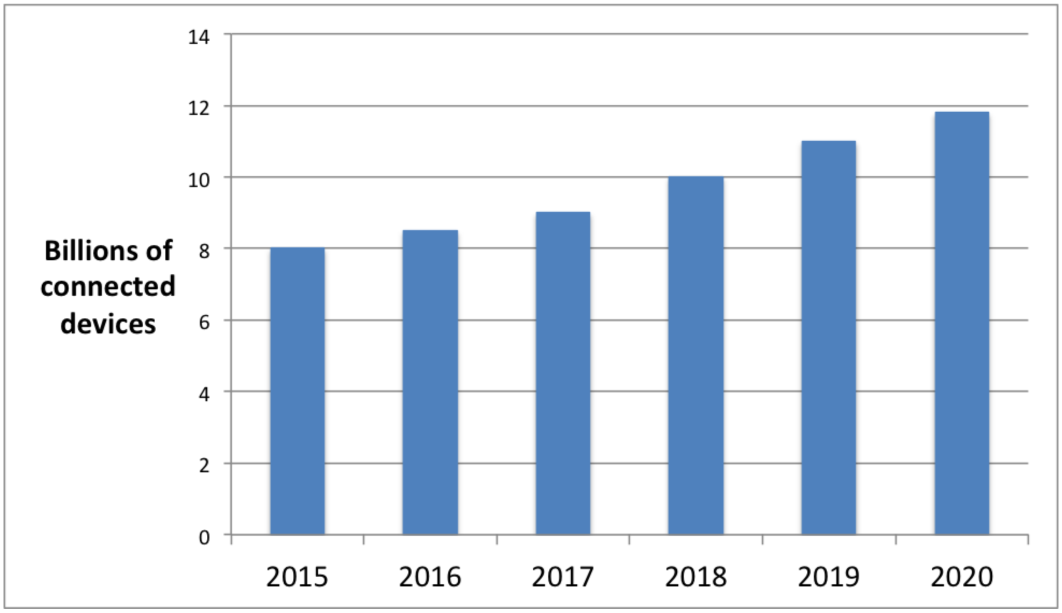

Figure 1.1: Cisco's Forecast of Connected Devices Evolution [2]

Interference is more severe in some frequency bands than others depending on licensing. Licensed bands are regulated bands where transmission is only allowed for specific users who pay a licensing fee to use an assigned channel within a frequency band. This ensures that the bands will not be subject to interference from other transmissions. Unlicensed bands lack this regulation. Transmission within unlicensed bands is allowed as long as the transmission initiated is based on the rules of transmission specific to the band. This is prevalent in the ISM bands (Industrial, Scientific and Medical) which consist of the bands centered at 915 MHz, 2.45 GHz and 5.8 GHz. The 900 MHz band has a very narrow bandwidth and is limited to applications such as home sensors, RFID readers and others. The 2.4 GHz is a congested band given the operation of Wi-Fi, Bluetooth, microwaves and others. In fact, the 2.4GHz ISM band consists of 13 overlapping channels spread equally over the frequencies with only three non-overlapping channels [5]. The 5 GHz, however, is less congested and gives 23 non-overlapping channels.

In this study, the focus is on the congested 2.4 GHz band and in particular the standards studied are the following:

- IEEE 802.15.4g which governs low-data rate and low-energy communication and enables large-scale applications such as the smart grid.
- IEEE 802.11 standards (or Wi-Fi) which govern wireless local area networking. Wi-Fi standards are important in examining interference with other standards given WiFi's dense prevalence in devices such as laptops, phones, etc. at a high transmission power using large packet sizes and high traffic [6].
- Bluetooth Low Energy version 4.0 under IEEE 802.15.1 or Bluetooth Smart in 2.4GHz band which governs low-power applications in the wireless personal area network of wearable devices, smart homes, healthcare, etc.

Given these standards, interference can exist in two forms: homogeneous interference or heterogenous interference. Homogeneous interference relates to the case where interference occurs within the same standard. For example, within IEEE 802.15.4g, there are three different physical layer specifications which could interfere with each other. Heterogenous interference, on the other hand, relates to the case where different standards occupy the same band and therefore interfere with each other. This is the case with overlapping channels pertaining to IEEE 802.11b/g, 802.11n, 802.15.4 and others.

This report addresses this well-recognized challenge of having different standards operating in a heterogeneous and homogeneous setting using the following:

- Simulation - IEEE 802.15.4g and IEEE 802.11 coexistence: Evaluating in simulation coexistence limits of different standards in a heterogeneous network.
- Setup - Bluetooth Low Energy version 4.0 under IEEE 802.15.1: Evaluating in a practical setting Bluetooth Low Energy (BLE) co-channel interference or homogeneous interference using an experimental setup built upon a multi-purpose, low-power radio which supports BLE.

Relating to the simulation portion of this report, previous work in this area included analytical analysis of coexistence of IEEE 802.15.4 with other systems in 2.4 GHz band such as IEEE 802.11 and Bluetooth in [7] or of IEEE 802.15.4 and IEEE 802.11b/g in [8]. This area is rich in studies as this topic is an evolving one adapting to the latest communication requirements and to the emergence of new standards and mechanisms to enable communication. The study in this report adds to the analysis the emerging IEEE 802.11ah standard which uses unlicensed bands to provide extended range Wi-Fi networks.

Relating to the testbed approach of this report, previous work such as [6], [9] and [10] includes analytic solutions and simulations to examine Bluetooth performance and throughput under co-channel interference. Other reports such as [11] use a radio to build a setup and run analysis of coexistence of BLE and Wi-Fi within 2.4GHz band. The approach in this report differs in the sense that the performance of BLE is optimized before the production of the chip. In other words, the work was done on the transceiver driver to optimize it for better BLE performance. This challenge has been an evolving one changing with the emergence of new radios and new performance requirements for different applications.

The rest of the report is organized as follows. Chapter 2 gives an overview of the standards that will be studied in this report along with the coexistence mechanisms that they have. Chapter 3 covers the first approach for evaluating standards coexistence using simulation and Chapter 4 addresses the second approach which relates to building testbeds. Chapter 5 highlights the results obtained from simulation and testbed experiments and Chapter 6 concludes this report.

Chapter 2

Standards Overview

In order to analyze the performance of standards under different co-existence scenarios, this chapter starts by examining the standards that this reports focuses on mainly BLE, IEEE 802.11 family and IEEE 802.15.4g. An overview of each standard is given along with physical layer specifications and co-existence mechanisms associated with the standards in a homogeneous and heterogeneous arrangement.

2.1 Bluetooth Low Energy (BLE)

2.1.1 Overview

BLE, a.k.a Bluetooth Smart, is a low-power wireless standard featured in Bluetooth version 4.0 specification. BLE, derived from classic Bluetooth, operates in the 2.4 GHz ISM band at 1 Mbps data rate. Similar to classic Bluetooth, BLE is based on frequency hopping (FHSS) which is a transmission method that consists of switching a carrier frequency among other frequency channels using a pseudorandom sequence known to the transmitter and receiver. BLE in fact hops among 40 Radio Frequency (RF) channels having a channel spacing of 2 MHz and classic Bluetooth hops among 79 RF channels having a channel spacing of 1 MHz.

Unlike classic Bluetooth, BLE is targeted for short-range, low-latency control and monitoring applications with coverage of tens of meters [12]. The reason behind being a low-power standard is that BLE slaves (which are BLE devices that accept incoming connection requests) initiate connections and therefore control their power consumption unlike a classic Bluetooth, where all slaves listen for incoming connections from masters (which are BLE devices that advertise connection requests to slaves) and therefore need to be on constant standby [12]. Table 2.1 summarizes all the differences between classic Bluetooth and BLE.

The physical layer specification of BLE requires Gaussian Frequency Shift Keying (GFSK) modulation with a modulation index falling in the range [0.45, 0.55]. GFSK uses a Gaussian filter to filter the signal before sending it to the modulator in order to make it smoother and specifies a modulation index given in Eq. 2.1

$$h = \frac{\Delta f}{R_b} \tag{2.1}$$

where Δf is the peak-to-peak frequency deviation and R_b is the bit rate.

The BLE receiver sensitivity is set to achieve a Bit Error Rate (BER) of 10^{-3} and is required to be better than or equal to -70 dBm.

Table 2.1: Bluetooth vs. BLE

Specification	Bluetooth	BLE
Speed (Mbps)	0.7	1
Range (m)	less than 30	50
RF Frequency band (GHz)	2.400 - 2.4835	2.400 - 2.4835
Channel Bandwidth (MHz)	1	2
Frequency Channels	79 channels	40 channels
Modulation	GFSK (modulation index 0.35) , $\pi/4$ DQPSK, 8DPSK	GFSK (modulation index 0.5)
Latency in data transfer between two devices	Approx. 100 ms	Approx. 3 ms
Spreading	FHSS	FHSS

2.1.2 Solutions for Coexistence

In order to alleviate interference caused by neighboring channels, BLE has some mechanisms implemented in frequency and time domains.

2.1.2.1 Channel Selection or Frequency Isolation

In order to alleviate heterogeneous coexistence with other standards, BLE employs Adaptive Frequency Hopping (AFH) mechanism which allows Bluetooth devices to select one of the available data channels for communication during a given time interval. It does so by marking channels as good, bad, or unknown [13]. To check for interference, BLE master periodically listens to bad channels. Bad channels in the frequency hopping pattern are replaced with good channels via a look-up table. In the absence of interference, the channel is marked as good and is removed from the look-up table.

2.1.2.2 Transmission Period Selection or Time Isolation

BLE implements Time Division Multiplexing (TDM) which is a coexistence method used to ensure to simultaneous operation of BLE with other coexisting standards such as Wi-Fi. TDM coordinates transmissions by dividing the time domain into several recurrent time slots of fixed length, one for each sub-channel.

2.2 IEEE 802.15.4g Smart Utility Network

2.2.1 Overview

IEEE 802.15.4g is an extension of IEEE 802.15.4 for Smart Utility Networks. It serves large-scale, low-power applications such as smart grid communications between home smart meters and utility data concentrators. IEEE 802.15.4g is made of a centralized coordinator that manages communication among devices [14] and consists of three physical layer designs that coexist:

- **Multi-rate Frequency Shift Keying:** This physical later provides good transmit power efficiency and uses Frequency Shift Keying (FSK). It uses convolutional coding as the Forward Error Correction (FEC) and supports data rates that range from 10 kbps to 400 kbps.

- **Multi-rate Orthogonal Frequency Division Multiplexing:** This physical layer provides higher data rates in channels with frequency selective fading. It uses Fast Fourier Transform (FFT) sizes of 128, 64, 32 and 16, with Binary Phase Shift Keying (BPSK), Quadrature Phase Shift Keying (QPSK) and 16-Quadrature Amplitude Modulation (16-QAM). It supports data rates that range from 50 kbps to 800 kbps.
- **Multi-rate Offset-Quadrature Phase Shift Keying:** This physical layer provides a more cost-effective and easier to design system. It uses raised cosine shaped O-QPSK and supports data rates that range from 12.5 kbps up to 500 kbps.

For all the above physical layer designs, IEEE 802.15.4 divides the 2.4 GHz ISM band into 16 non-overlapping channels, which are 5 MHz apart with a coverage range up to 100 m.

2.2.2 Solutions for Coexistence

In order to alleviate the interference of coexistence within IEEE 802.15.4g physical layers and IEEE 802.15.4g with other standards, mechanisms for spread spectrum, channel access, and physical layer management are implemented.

2.2.2.1 Multi-PHY Management (MPM)

To manage the homogenous interference within the three PHY layers of IEEE 802.15.4g, a mechanism, MPM, is defined [14]. Within MPM, the coordinators scan for an interference signal. If detected, the coordinators know there is another transmission on the channel and therefore try to use an unoccupied channel.

Since the three different physical layer designs don't recognize each other's signals, MPM is used to ensure a common signal design called the Common Signaling Mode (CSM). MPM consists of the following [15]:

- A common signaling, CSM, is used to enable communication among different physical layer designs.
- A MAC frame, Enhanced Beacon (EB), is used to enable coexistence.
- Other MAC procedures are used for discovery and synchronization among different networks.

Given the above, a network coordinator, which operates a network, informs potential networks of an existing network using the channel through periodically sending EB frames.

2.2.2.2 Spread Spectrum

To transmit over more bandwidth using more frequencies and less power per frequency, Direct Sequence Spread Spectrum (DSSS) is used. DSS uses a chip sequence, which is a pseudorandom sequence sent at a high rate, to modulate the carrier signal.

2.2.2.3 Channel Access

To manage accessing multiple channels, IEEE 802.15.4g uses Carrier Sense Multiple Access/ Collision Avoidance (CSMA/CA) which does not require synchronization between devices and employs a simple listen before talking strategy. Before transmitting, devices carry out Clear Channel Assessment (CCA) to check if the channel is being used. CCA can be of the form of detecting if energy is above a certain threshold or the presence of a signal such as CSM [14].

2.3 IEEE 802.11 Family

2.3.1 Overview

IEEE 802.11 governs communication between a wireless client and an access point, or between two or more wireless clients. IEEE 802.11 was amended over the years as summarized in Table 2.2.

IEEE 802.11b which operates in 2.4 GHz band and IEEE 802.11a, which operates in the 5 GHz band, were the first two standards in the IEEE 802.11 family. IEEE 802.11b uses BPSK and QPSK modulation and covers a range of 100 m [16]. IEEE 802.11a and later IEEE 802.11g use orthogonal frequency division multiplexing (OFDM) in 5 GHz and 2.4 GHz ISM bands, respectively, to achieve speeds of up to 54 Mbps. IEEE 802.11n emerged and quadrupled the throughput compared to IEEE 802.11a/g networks. It supports up to 4 antennas which allows for better spectral efficiency and increased reliability. After IEEE 802.11n, IEEE 802.11ac and IEEE 802.11ad were developed to

Table 2.2: IEEE 802.11 Family [1]

Standard	**Description**
IEEE 802.11	WLAN; up to 2 Mb/s; 2.4 GHz
IEEE 802.11a (Wi-Fi5)	WLAN; up to 54 Mb/s; 5 GHz
IEEE 802.11b (Wi-Fi)	WLAN; up to 11 Mb/s; 5 GHz
IEEE 802.11g	WLAN; up to 54 Mb/s; 2.4 GHz
IEEE 802.11e	New distribution functions for QoS
IEEE 802.11ah	cost-effective and large scale wireless networks
IEEE 802.11f	Inter-AP Protocol
IEEE 802.11h	Use of the 5 GHz band in Europe

support high definition streaming video, voice over IP calls, web page delivery, and fast data transfers.

IEEE 802.11ah, is another standard that is intended for cost-effective and large scale wireless networks with a range of 100 -1000 m. IEEE 802.11ah has a star topology and channel bandwidth taking one of the following values: 1, 2, 4, 8 or 16 MHz. The modulation used is BPSK, QPSK, or 16 to 256 QAM [17]. IEEE 802.11ah physical layer has two modes [18]: when the channel bandwidth is greater than or equal to 2 MHz and when the channel bandwidth is 1 MHz.

2.3.2 Solutions for Coexistence

Standards within the Wi-Fi family have inherent coexistence mechanisms that are essential for coordinating the transmission and communication within the 2.4 GHz band shared with other IEEE standards. These mechanisms are mainly dynamic channel selection and adaptive packet fragmentation.

2.3.2.1 Dynamic Channel Selection

Wi-Fi employs a collision avoidance algorithm that listens for a quiet channel before transmitting. To determine the channel to use for transmission there are several methods [16]:

- Using Packet Error Rate (PER) measurements in order to choose the channels with lower PER.
- Received Signal Strength (RSS) measurements in order to choose the channels with the least interferer RSS.
- Signal to Noise (SNR) measurements in order to choose the channels with the highest SNR.

2.3.2.2 Adaptive Packet Fragmentation

Another mechanism to combat interference involving Wi-Fi is to fragment packets into smaller ones. Although this increases the overhead and decreases the throughput, this technique increases throughput in the scenario of interference [19] because a decrease in the packet length decreases the probability of interference. Fragmentation consists of monitoring PER and overhead associated with each packet to adjust fragmentation accordingly [16].

2.4 Summary

To summarize, Table 2.3 reveals the relevant properties of the standards discussed in this chapter.

Table 2.3: Standards Summary

IEEE Standards	**Frequency Channels**	**Channel Bandwidth (MHz)**	**Range (m)**	**Speed (Mbps)**	**Modulation**
Bluetooth - LE	40	2	50	1	GFSK
802.15.4g	16	500	100	0.5	FSK, QPSK, BPSK, 16 - QAM
802.11ah	80, 40, 20, 10, or 5	1, 2, 4, 8, or 16	100 -1000	0.15	BPSK, QPSK, or 16 to 256 QAM

Chapter 3

Heterogeneous Interference Simulation

Given the standards overview illustrated in Chapter 2, this chapter sets the stage for the first part of this report which is the simulation. Different coexistence scenarios between different standards given in Chapter 2 are simulated to analyze the communication performance. This chapter explains the simulation setting used in terms of interference scenario, physical separation between transceivers, models of path loss and interference and finally error analysis which is based on studies in [14], [20], and [21].

3.1 Interference Scenario

The interference scenario consists of the the receiver and transmitter of the victim or intended communication as well as the transmitter of the interferer. As shown in Fig. 3.1, the receiver of the victim is at a distance d_D from the transmitter of the victim and at a distance d_U from the transmitter of the interferer [14], [20], [21]. The transmitter and receiver of the victim are referred to as TX_v (with transmit power P_{Tv} and transmit gain G_{Tv}) and RX_v respectively while the interfering transmitter and receiver are referred to as TX_i (with transmit power P_{Ti} and transmit gain G_{Ti}) and RX_i respectively.

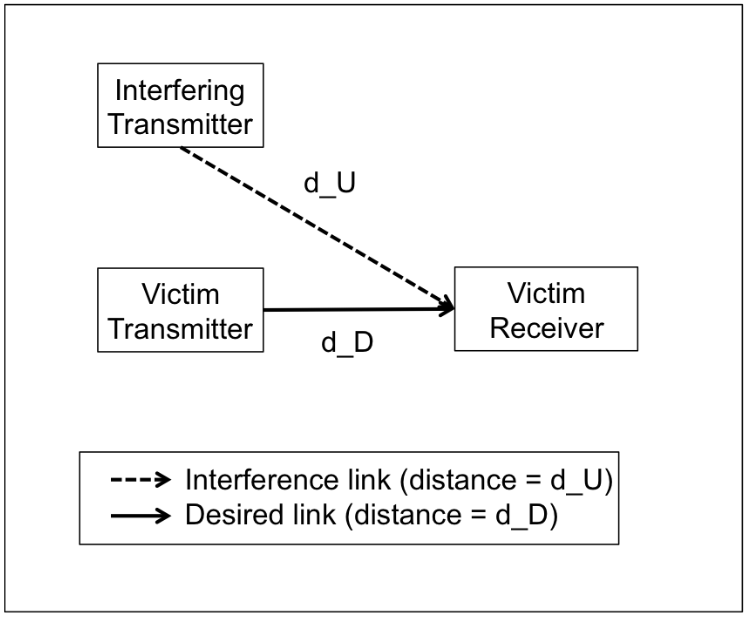

Figure 3.1: Interference Scenario

3.2 Avoidance based on Physical Separation

Given the model in Fig 3.1, this section analyzes the receiver victim-interferer transmitter physical separation (d_U), path loss (PL) models along the connection link and interference models. These main models follow.

3.2.1 Path Loss Models

The path loss model along the connection link between the victim receiver and the interferer transmitter follows the Hata outdoor large-zone typical urban model [20]. This model is given by the following empirical formula based only on measurements for carrier frequencies greater than 300 MHz and adopted in [14] and [20]:

$$\begin{aligned}\mathrm{PL}^{dB}(d_D) = 69.55 &+ 26.16\log(f_c)\\ &+ (44.9 - 6.55\log(h_{TXv}))\log(d_D)\\ &- 13.82\log(h_{RXv} - g(h_{RXv}))\end{aligned}$$

Here, f_c is the carrier frequency, h_{TXv} and h_{RXv} are the heights of the transmitter and receiver, respectively, d_D is the communication range, and $g(h_{RXv})$ is the height correction factor defined as follows:

$$g(h_{RXv}) = 3.2\left(\log(11.75 \cdot h_{RXv})\right)^2 - 4.97 \tag{3.1}$$

3.2.2 Interference Model

Based on Fig. 3.1, the victim receiver receives a signal generated by victim transmitter located at a distance d_D from it in addition to a signal generated by an interfering transmitter located at a distance d_U from it [14]. To evaluate the communication performance of the intended communication between the receiver and transmitter of the victim, the desired-to-undesired ratio (DUR) is used. DUR is the ratio between the desired power from the victim transmitter $P_{(Tv,Rv)}$ and the undesired power from the interfering transmitter $P_{(Ti,Rv)}$. DUR will be used as the signal-to-interference ratio of the victim system to evaluate its performance in the presence of an interferer that introduces an undesired signal. DUR is defined as follows.

$$\text{DUR}^{dB} = P_{Tv,Rv} - P_{Ti,Rv} \tag{3.2}$$

where

$$P_{Tv,Rv}(d_D) = P_{Tv} + G_{Tv} + G_{Rv} - PL(d_D) \tag{3.3}$$

and

$$P_{Ti,Rv}(d_U) = P_{Ti} + G_{Tv} + G_{Rv} - PL(d_U) \tag{3.4}$$

3.2.3 Error Analysis

In order to complete the analysis, the signal to noise ratio at the victim receiver, SNR, and the Frame Error Rate, FER, are calculated as follows.

$$\text{SNR}^{dB}(d_D) = 10\log\left(\frac{P_{signal}}{P_{noise}}\right) = P_{Tv} + G_{Tv} + G_{Rv} - S_{rec} - PL(d_D) \tag{3.5}$$

where S_{rec} is the receiver sensitivity.

FER is obtained as shown in Fig. 3.2 using:

$$\text{FER} = 1 - (1 - \text{BER})^{L_f} \tag{3.6}$$

where L_f is the frame length. To evaluate the performance in Chapter 5, we set an FER to our target FER (1%) and we find the desired separation required to achieve it.

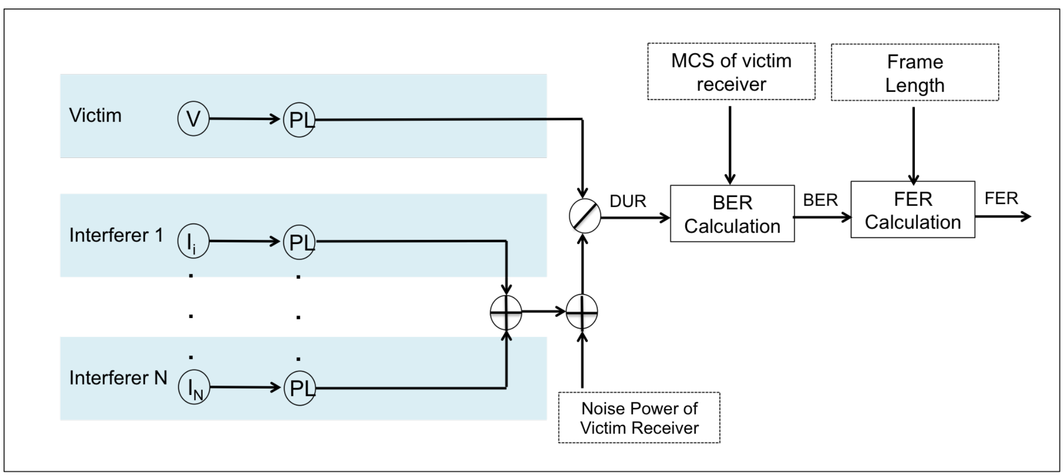

Figure 3.2: BER and DUR calculation

Chapter 4

Homogeneous Interference Measurement

The previous chapter explains the first approach used in this report to evaluate performance of standards under coexistence. The approach was through simulation and was explained in terms of coexistence scenario, path loss, and interference models in addition to performance metrics. In this chapter, the second approach used in this report for performance evaluation is explained. This approach is through testbeds built to run experiments using over-the-air signals.

4.1 Setup

To evaluate the practical effect of interference, signals over the air mixed with interfering signals are used to evaluate their reception at the intended receiver. As such, I worked on an experiment using a BLE transceiver to evaluate co-channel interference within BLE under different settings.

The setup consists of two parts:

- Selectivity setup: It consists of sending to the transceiver a desired BLE signal along with an interference BLE signal which varies in transmission power. This aims to check how selective the transceiver is in detecting the desired signal in presence of interference.

- Sensitivity setup: It consists of sending to the transceiver the desired signal only which varies in transmission power. This aim is to check the power at which the receiver is sensitive and below which it doesn't meet the required performance of reception.

To build the setups, I used the hardware components and software tools that are listed in Tables 4.1 and 4.2 respectively.

Table 4.1: Hardware Testbed Tools

Hardware Tool	**Description**
R&S SMBV100A	Vector Signal Generator programmed to generate interference RF signal
Agilent MXG	Vector Signal Generator programmed to generate desired RF signal
BLE Transceiver	Transceiver
HP DC Power Supply	used to power the transceiver
Jlink	used to interface the board with the laptop
Laptop	used to run the transceiver code and gathering statistics
Signal Mixer	used to mix the interference with the desired RF signal

Table 4.2: Software Testbed Tools

Software Tool	Description
IAR Workbench	Workbench used to run and debug the transceiver code
Microsoft Excel	Worksheet used to dump the data and evaluate them
MATLAB	Scripting used to manipulate data and generate plots

4.1.1 Selectivity Setup

The selectivity setup consists of all the components listed in Table 4.1 which are connected as shown in Fig. 4.1. Both the MXG and SMBV are programmed to generate the respective signals and the process of reaching the stage of a fully functioning setup required a lot of debugging on the hardware and software side.

On the board, there are two pins that are critical to the functioning of the setup. These pins function as triggers: one pin triggers the MXG to transmit 2500 packets of BLE to the board and another pin triggers the SMBV to step to another power level of the interference signal and transmit it. The desired RF signal has a length of 367ms generated 2500 times at -67 dBm every time the MXG is triggered. The interference signal is generated by SMBV at a power level sweeping from -100 dBm to 10 dBm with 2 dBm steps. Every time the SMBV is triggered the power level changes by one step.

The interference signal and the desired signal are combined and sent to

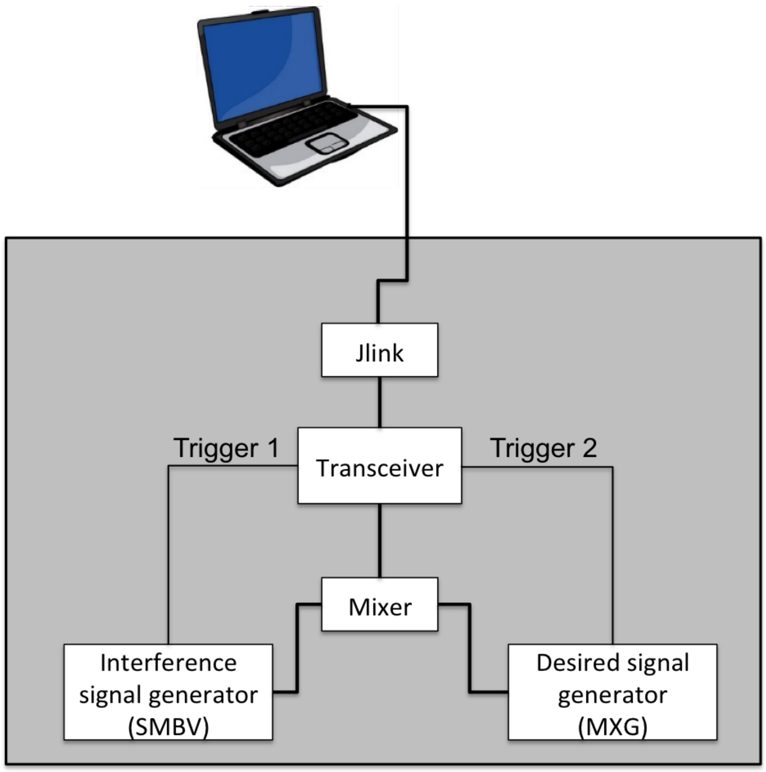

Figure 4.1: Selectivity Setup

the transceiver. At this point, running the code in IAR Embedded Workbench, statistics are collected such as the number of good, number of bad and number of missing packets out of the 2500 packets at each interference signal power level.

4.1.2 Sensitivity Setup

The sensitivity setup is similar to the selectivity setup except that in this case the interference signal is removed and only the desired RF signal is

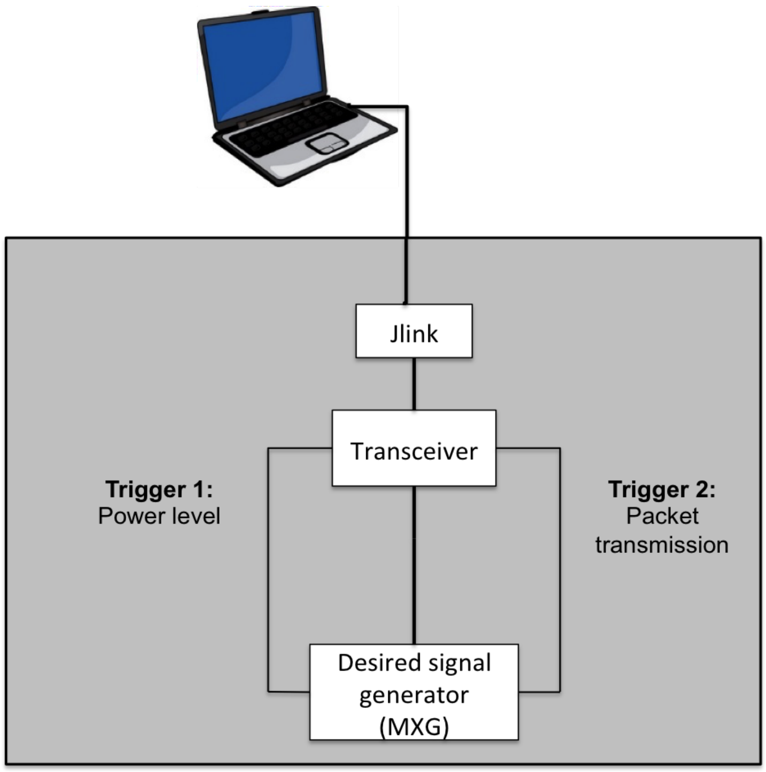

Figure 4.2: Sensitivity Setup

sent to the transceiver as shown in Fig.4.2. In this case, there are two pins on the board used as triggers: one triggers the MXG to generate 2500 BLE packets and the other triggers the MXG to step into another power level of transmission which range from -100 dBm to 10 dBm in 2 dBm steps.

Similarly, IAR Embedded Workbench is used to capture the number of good, number of bad and number of missing packets out of the 2500 packets at signal power level.

4.2 Experiments

Having the above two setups, experiments were designed in order to calibrate the transceiver to meet certain performance metrics in order to reduce the interference within BLE channels. The performance metrics focussed on are the following:

- PER which is aimed to be less 30.8% (which corresponds to 1% Bit Error Rate specific for the BLE standard). PER is calculated based on the statistics collected as follows:

$$\text{PER} = \frac{1 - n_{\text{good}}}{n_{\text{total}}} * 100 \tag{4.1}$$

  Here, n_{good} is number of good packets received and n_{total} is total number of packets which is 2500.

- Carrier to interference (C/I) ratio which is targeted to be less than $-50dBm$. C/I is calculated as follows:

$$\text{C/I} = P^{dBm}_{\text{desired}} - P^{dBm}_{\text{interference}} \tag{4.2}$$

  where P^{dBm}_{desired} in the selectivity setup is set to -67 dBm and $P^{dBm}_{\text{interference}}$ is the interference power level at which PER exceeds the 30.8% target.

Having these metrics set, experiments were run under different settings in order to evaluate C/I and the level of interference and calibrate the board to reduce it. Calibration was critical for the Automatic Gain Control (AGC)

Table 4.3: Setup Experiment Settings

Setting	**Value**
Modulation	GFSK (time-bandwidth product of 0.5 and 0.3 and modulation index of 0.5)
Board Clock Frequency (MHz)	32, 26
Bit Rate (kbps)	250, 500, 1000
Interference Frequency Offset (MHz)	2, 3, 5, 7, 10
AGC Settings	5 different settings
DC Trim functions	3 different functions

value and DC Trim functions at the initialization step of the transceiver which determine the first estimate of the signal received.

Table 4.3 summarized the settings under which the statistics where run.

Chapter 5

Results

After explaining in the previous two chapters the two approaches (simulation and testbed experiments) that are used to evaluate the performance of standards with coexistence, this chapter displays the results obtained from these two approaches.

5.1 Simulation

Simulations were run to evaluate coexistence within the three PHY modes of IEEE 802.15.4g in addition to different coexistence scenario performances within different standards. Also the performance of the physical distance separation mechanism discussed in Chapter 4 is evaluated.

5.1.1 Coexistence within the three PHY modes of IEEE 802.15.4g

Given the three different PHY layer designs within IEEE 802.15.4g explained in Chapter 2, Figs. 5.1a and 5.1b display BER and FER plots of these physical layer modes based on the parameters in Table 5.1.

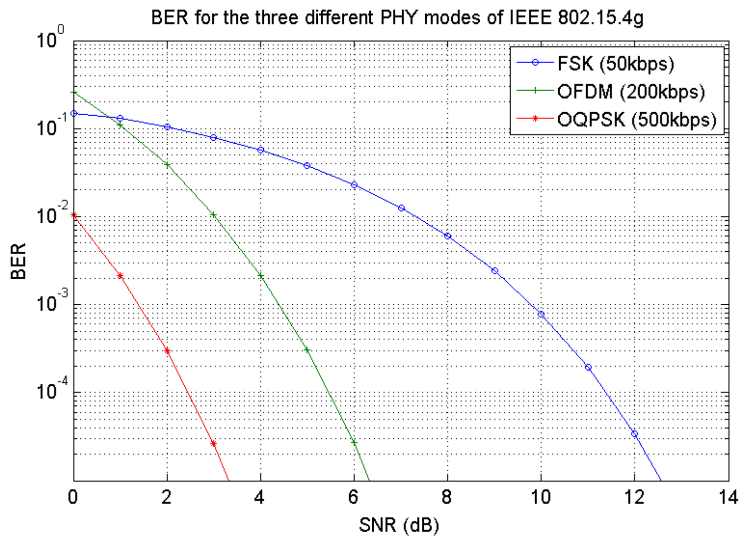

(a) BER for IEEE 802.15.4g PHY Modes

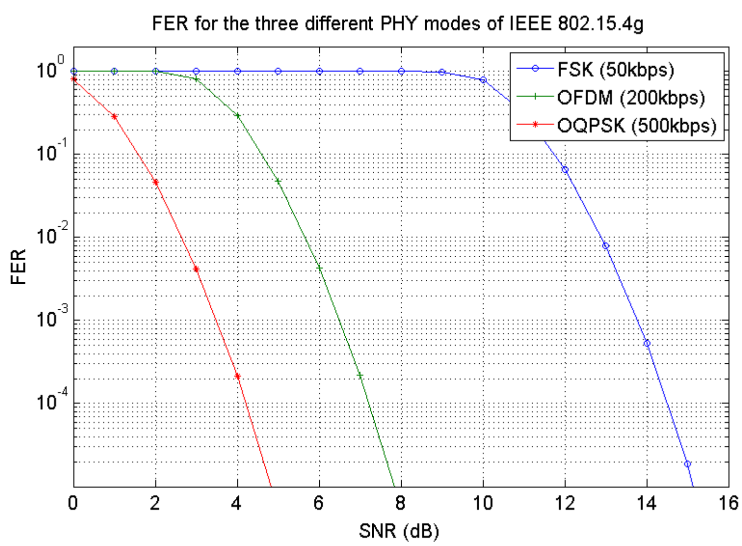

(b) FER for IEEE 802.15.4g PHY Modes

Figure 5.1: BER and FER for IEEE 802.15.4g PHY Modes

Table 5.1: IEEE 802.15.4g Physical Layer Modes

PHY	MR-FSK	MR-OFDM	MR-OQPSK
RX Bandwidth (kHz)	200	200	2000
TX Power (dBm)	0	0	0
Frame Length (octets)	250	20	20
RX Sensitivity (dBm)	-90	-100	-90
PHY Mode	500kbps FSK	200kbps QPSK CC R_{FEC}=0.5	500kbps O-QPSK CC R_{FEC}=0.5 (8,4) DSSS

5.1.2 Coexistence Scenario (I): IEEE 802.15.4g and 802.11ah

In this coexistence scenario, IEEE 802.15.4g has a transmitter interfering with the intended communication between an IEEE 802.11ah transmitter and receiver. The joint parameters of the transmitters and receivers of the interferer and victim are given by Table 5.2.

Table 5.2: Interferer IEEE 802.15.4g Parameters

TX transmit power (dBm)	0
RX bandwidth (kHz)	200

The BER and FER plots are given in Fig. 5.2. Also, given in Figs. 5.3a and 5.3b, for FER of 1%, a distance of about 11 m is required to separate the interfering transmitter of IEEE 802.15.4g FSK from the victim receiver IEEE 802.11ah and a distance of 8.5 to 9.5m is required to separate the interfering transmitter of IEEE 802.15.4g OQPSK from the victim receiver IEEE 802.11ah based on parameters in Table 5.3.

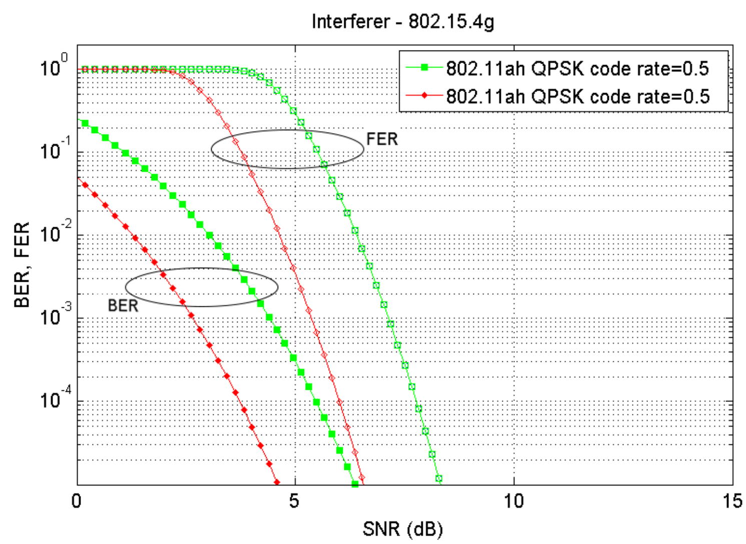

Figure 5.2: BER (shaded markers) and FER (unshaded markers) vs. SNR for 802.11ah victim in the presence of 802.15.4g interferer

Table 5.3: Interferer IEEE 802.15.4g OQPSK Parameters

TX transmit power (dBm)	0
RX bandwidth (kHz)	2000

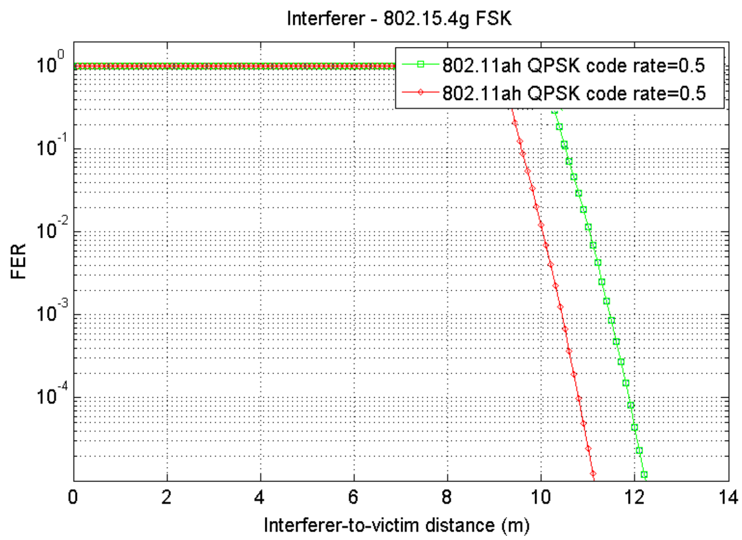

(a) FER vs. distance between 802.15.4g FSK (interferer) and the physical layer modes of 802.11ah victim receiver

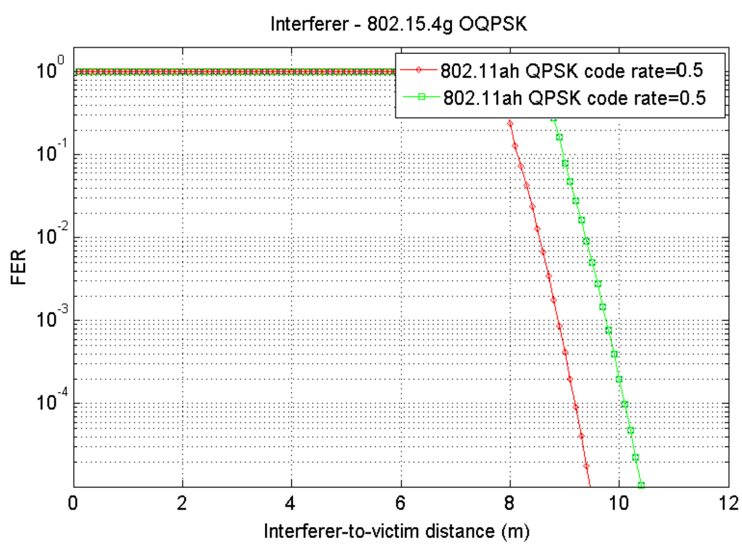

(b) FER vs. distance between 802.15.4g OQPSK (interferer) and the physical layer modes of 802.11ah victim receiver

Figure 5.3: FER vs. distance between IEEE 802.15.4g interferer and physical layer modes of 802.11ah victim receiver

For a larger distance, path loss and interferer received power at the victim receiver are plotted vs. interferer-to-victim distance for IEEE 802.15.4g OQPSK in Fig. 5.4.

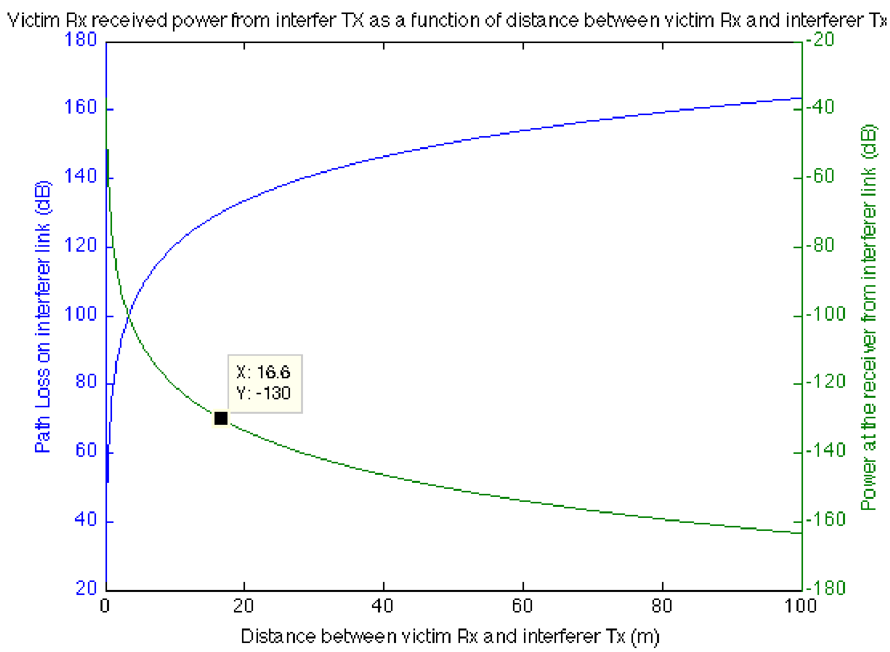

Figure 5.4: Victim Rx received power from 802.15.4g OFDM interferer TX vs. distance between victim Rx and interferer Tx

Since the receiver sensitivity for IEEE 802.15.4g is -120dB (-90dBm), this corresponds to a distance separation of 9.7m. For OFDM, the sensitivity is -130dB which corresponds to 16.6m. As for OQPSK, the receiver sensitivity is -130dB (-100dBm) which corresponds to a distance separation of 16.9m as shown in Fig. 5.4. This allows us to better estimate the distance separation needed between IEEE 802.15.4g tranceivers that interfere with the victim

IEEE 802.11ah receiver.

5.1.3 Coexistence Scenario (II): IEEE 802.15.4g and 802.11

IEEE 802 systems (such as 802.11b/g , 802.11n, 802.15, 802.15.3 and 802.15.4) interfere in the communication between an IEEE 802.15.4g transmitter and receiver if all are in the same transmission band. BER and FER plots are given in Figs. 5.5a and 5.5b respectively. These plots show that for FER of 1%, a distance of about 22 (FSK) or 33m (OFDM or OQPSK) is required to separate the interferers transmitter from the victim receiver.

Table 5.4 has the parameters of the IEEE 802 systems used in these simulations.

Table 5.4: Interferers IEEE 802 Parameters

	802.11ah	802.15.4c	802.15.4
TX transmit power (dBm)	0	14	0
RX bandwidth (Hz)	1M	2M	2M

5.1.4 Critical Distance Separation

The distance below which the interferer causes performance degradation greater than that required by the IEEE 802.11ah and 802.15.4g standards, in this case 1%, is referred to as the critical distance. In the previous section, the physical layers of IEEE 802.15.4g are plotted and two scenarios of coexistence are studied to establish the critical distance between IEEE 802.15.4g

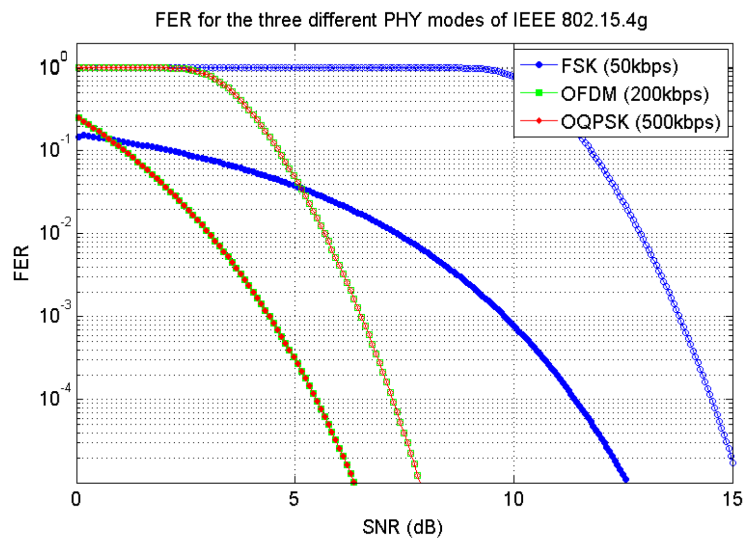

(a) BER (shaded markers) and FER (unshaded markers) vs. SNR for 802.15.4g victim in the presence of 802.11 interferers

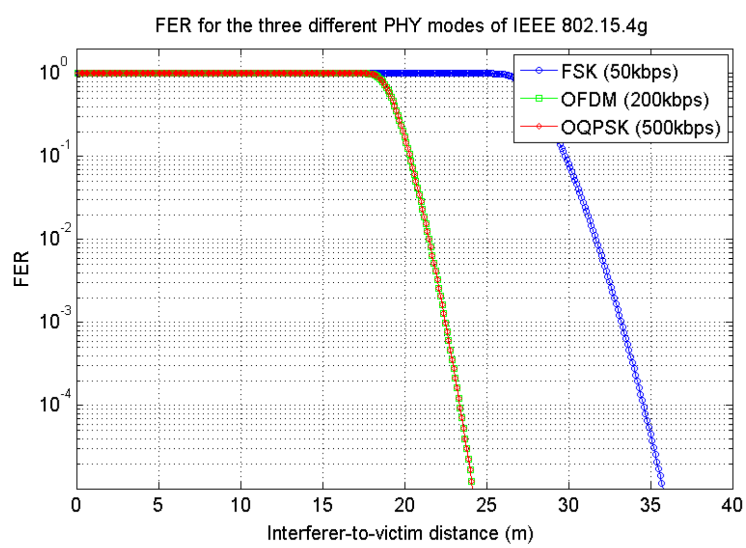

(b) FER vs. distance between 802.15.4g OQPSK (interferer) and the physical layer modes of 802.11ah victim receiver

Figure 5.5: BER and FER under different scenarios

and IEEE 802.11ah along with other 802.11 systems.

From the figures above we can obtain the critical distance range in Table 5.5 which adds IEEE 802.11ah to the table of established critical distances in [14], [20] and [22].

Table 5.5: Critical Victim - Interferer Distance

Interferer (s)	Victim	Victim Required FER (1%)	d_{cri}(m)
802.15.4g FSK	802.11ah	1	9.7
802.15.4g OFDM	802.11ah	1	16.9
802.15.4g OQPSK	802.11ah	1	16.9
802.11ah and 802.11b/g and 802.11n	802.15.4g FSK	1	33
	802.15.4g OFDM	1	22
	802.15.4g OQPSK	1	22

5.2 Measurement

Using the setups built for evaluating BLE co-channel interference through calibrating the transceiver, I ran different experiments. First, I started with running the BLE desired signal with interference channels at 2, 3, 5, 7, 10 MHz offsets. Going through these runs and trying different boards, I was able to narrow down the study to using the 2 and 3 MHz interference offsets because they displayed a more sever performance deterioration than the rest given that they are closer to the desired frequency of transmission 2.402 GHz. After narrowing down the interference signals that I will use, I moved on to calibrating the Automatic Gain Control threshold value which is critical for the functioning of the transceiver and to its performance. I tried a range of values for the AGC threshold value on a set of about 10 boards socketed and soldered which helped me pick the value that allowed for PER $< 30.8\%$ and C/I > -50 dBm. Since some boards still didn't perform up to the target specifications of PER and C/I, I varied other parameters and added calibration at the initialization of the board to calibrate the DC step. Three trim functions were compared for this calibration and the one with the best running time and performance was chosen. Results are summarized in Tables 5.6 and 5.7 similar to those shared in a poster presented at TWS 2016.

Table 5.6: Sensitivity for BLE GFSK (BT = 0.5, h = 0.5) at 2.404 GHz

Data Rate (kbps)	Sensitivity Level (dBm)
1000	-94
500	-98
250	-99

Table 5.7: Selectivity for BLE GFSK (BT = 0.5, h = 0.5) at 2.404 GHz

Interferer Frequency Offset (MHz)	C/I Ratio (dB)	Interference power where PER > 30.8% (dB)
-3	-54	-13.5
-2	-47	-19.5
3	-47	-19.5
2	-55	-11.5

Chapter 6

Conclusion

With the growing interest in the Internet of Things, unlicensed frequency bands are becoming congested by an increasing number of wireless devices governed by different standards. As a result, the communication performance between transmitters and their intended receivers deteriorates. This report targets the evaluation of coexistence for selected Wireless Personal Area Network standards using simulation and experimental approaches. The challenging aspect of it for me was the testbed portion were I was trying to build a full system and make sure it works. I learnt hands-on skills in debugging hardware using tools such as signal analyzers and logic analyzers, programming two different instruments for signal vector generation and understanding software/hardware interactions. Going through the process, I appreciated the precision, problem-solving and collaboration that is put into testing and calibrating a board and I feel contended that the board I worked will be used in some devices I use everyday.

Bibliography

[1] "Bluetooth vs BLE-difference between Bluetooth and BLE(Bluetooth Low Energy)," *RF Wireless World*, 2012.

[2] Cisco, "Cisco Visual Networking Index: Global Mobile Data Traffic Forecast Update, 20152020 White Paper," Feb. 2016.

[3] C. Boano, T. Voigt, C. Noda, K. Romer, and M. Zungia, "Jamlab: Augmenting sensornet testbeds with realistic and controlled interference generation," *International Conference on Information Processing in Sensor Networks*, pp. 175–186, April 2011.

[4] M. Bertocco, G. Gamba, and A. Sona, "Is csma/ca really efficient against interference in a wireless control system? an experimental answer," in *IEEE International Conference on Emerging Technologies and Factory Automation*, Sept 2008, pp. 885–892.

[5] R. Nilsson, "What is the Difference Between 2.4GHz and 5GHz Wireless LAN in Industrial Applications?" *CEO connectBlue*. [Online]. Available: http://www.connectblue.com/press/articles/what-is-the-difference-between-24ghz-and-5ghz-wireless-lan-in-industrial-\\applications/

[6] T. Hayajneh, G. Almashaqbeh, S. Ullah, and A. V. Vasilakos, "A survey of wireless technologies coexistence in WBAN: analysis and open research issues," *Wireless Networks*, vol. 20, no. 8, pp. 2165–2199, 2014.

[7] A. Sikora and V. F. Groza, "Coexistence of IEEE802.15.4 with other Systems in the 2.4 GHz-ISM-Band," in *2005 IEEE Instrumentation and Measurement Technology Conference Proceedings*, vol. 3, May 2005, pp. 1786–1791.

[8] W. Yuan, X. Wang, and J. P. M. G. Linnartz, "A Coexistence Model of IEEE 802.15.4 and IEEE 802.11b/g," in *2007 14th IEEE Symposium on Communications and Vehicular Technology in the Benelux*, Nov 2007, pp. 1–5.

[9] S. Souissi and E. F. Meihofer, "Performance evaluation of a Bluetooth network in the presence of adjacent and co-channel interference," in *Emerging Technologies Symposium: Broadband, Wireless Internet Access, IEEE*, April 2000, p. 6 pp.

[10] G. Sun, G. Qiao, and B. Xu, "Link characteristics measuring in 2.4 GHz body area sensor networks," *International Journal of Distributed Sensor Networks*, vol. 2012, 2012.

[11] "Wireless Coexistence in the 2.4 GHz Band," *Freescale Semiconductor Inc. Application Note*, no. 1, Sept. 2015. [Online]. Available: http://www.nxp.com/assets/documents/data/en/application-notes/AN5185.pdf?&pspll=1

[12] J. P. Carles Gomez, Joaquim Oller, "Overview and Evaluation of Bluetooth Low Energy: An Emerging Low-Power Wireless Technology," *Sensors*, p. 1173411753, Aug 2012.

[13] R. Kandiar, "Interference Mitigation Challenges and Solutions in the 2.4 to 2.5-GHz ISM Band," *Cypress Semiconductors*, 2014. [Online]. Available: http://www.cypress.com/file/131521/download

[14] C. S. Sum, "TG4g Coexistence Assurance Document," *IEEE P802.15 Wireless Personal Area Networks*, April 2011.

[15] C. S. Sum, M. A. Rahman, C. Sun, F. Kojima, and H. Harada, "Performance of common signaling mode for Multi-PHY management in smart utility networks," in *IEEE International Conference on Communications Workshops (ICC)*, June 2011, pp. 1–5.

[16] P. Matthew and B. Shoemake, "Wi-Fi (IEEE 802.11b) and Bluetooth Coexistence Issues and Solutions for the 2.4 GHz ISM Band," *Texas Instruments*, Feb 2011.

[17] T. Adame, A. Bel, B. Bellalta, J. Barcelo, and M. Oliver, "IEEE 802.11ah: The WiFi Approach for M2M Communications," *IEEE Wireless Comm.*, vol. 21, no. 6, pp. 144 – 152, Dec. 2014.

[18] W. Sun, M. Choi, and S. Choi, "IEEE 802.11ah: A Long Range 802.11 WLAN at Sub 1 GHz," *Journal of Information and Communication Technology Standardization*, Apr. 2013.

[19] M. B. Shoemake and P. Lowry, "IEEE 802.11b and Bluetooth Coexistence Testing Results," *IEEE 802.15-01/084*, Jan 2001.

[20] C. S. Sum, F. Kojima, and H. Harada, "Coexistence of Homogeneous and Heterogeneous Systems for IEEE 802.15.4g Smart Utility Networks," *IEEE Int. Symp. on Dynamic Spectrum Access Networks*, pp. 510 – 520, May 2011.

[21] R. Ma, W. Meng, H. H. Chen, and Y. R. Huang, "Coexistence of Smart Utility Networks and WLAN/ZigBee in Smart Grid," *IEEE Smart Grid Comm. Symp.*, pp. 211 – 216, Nov. 2012.

[22] C. S. Sum, M. A. Rahman, L. Lu, F. Kojima, and H. Harada, "On Communication and Interference Range of IEEE 802.15.4g Smart Utility Networks," *IEEE Wireless Comm. and Networking Conf.: PHY and Fundamentals*, pp. 1169 – 1174, April 2012.

Vita

Ghadi Sebaali was born in Jal El Dib, Lebanon on 19 September 1992. She attended Saint Joseph School, Cornet Chehwan where she graduated valedictorian in 2010. Ghadi received the Bachelor of Engineering degree in Computer and Communication Engineering from the American University of Beirut in 2014 after which she enrolled in the graduate Electrical and Computer Engineering program at The University of Texas at Austin under the supervision of Prof. Brian L. Evans. During her graduate studies, she interned at Freescale Semiconductors and NXP Semiconductors.

Permanent address: 3316 Guadalupe Street
Austin, Texas 78705

This report was typeset with LaTeX[†] by the author.

[†]LaTeX is a document preparation system developed by Leslie Lamport as a special version of Donald Knuth's TeX Program.